Learning Kinematic Models for Articulated Objects

Jürgen Sturm[1] **Vijay Pradeep**[2] **Cyrill Stachniss**[1]
Christian Plagemann[3] **Kurt Konolige**[2] **Wolfram Burgard**[1]

[1] *Univ. of Freiburg, Dept. of Computer Science, D-79110 Freiburg, Germany*
[2] *Willow Garage, Inc., 68 Willow Road, Menlo Park, CA 94025*
[3] *Stanford University, CS Dept., 353 Serra Mall, Stanford, CA 94305-9010* *

Abstract

Robots operating in home environments must be able to interact with articulated objects such as doors or drawers. Ideally, robots are able to autonomously infer articulation models by observation. In this paper, we present an approach to learn kinematic models by inferring the connectivity of rigid parts and the articulation models for the corresponding links. Our method uses a mixture of parameterized and parameter-free (Gaussian process) representations and finds low-dimensional manifolds that provide the best explanation of the given observations. Our approach has been implemented and evaluated using real data obtained in various realistic home environment settings.

1 Introduction

Home environments are envisioned as one of the key application areas for service robots. Robots operating in such environments are typically faced with a variety objects they have to deal with or to manipulate to fulfill a given task. Furthermore, many objects are not rigid since they have moving parts such as drawers or doors. Understanding the spatial movements of parts of such objects is essential for service robots to allow them to plan relevant actions such as door-opening trajectories. In this paper, we investigate the problem of learning kinematic models of articulated objects from observations. As an illustrating example, consider Fig. 1 which depicts two examples for observations of the door of a microwave oven and a learned, one-dimensional description of the door motion.

Our problem can be formulated as follows: Given a sequence of locations from observed objects parts, learn a compact kinematic model describing the *whole* articulated object. This kinematic model has to define (i) the connectivity between the parts, (ii) the dimensionality of the latent (not observed) actuation space of the object, and (iii) a kinematic function between different body parts in a generative way allowing a robot to reason also about unseen configurations.

*This work has partly been supported by the DFG under contract number SFB/TR-8 and the EU under FP6-IST-045388 (INDIGO).

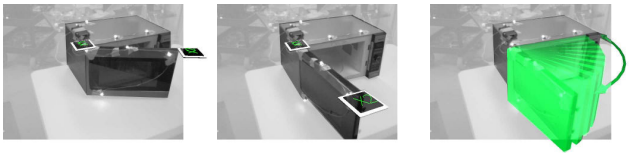

Figure 1: Left and middle: examples for observations of a moving door of a microwave oven. Right: visualization of the kinematic model of the door learned by our approach.

The contribution of this paper is a novel approach for learning such models based only on observations. Our method is able to robustly detect the connectivity of the rigid parts of the object and to estimate accurate articulation models from a candidate set. It allows for selecting the best model among parametric, expert-designed transformation templates (rotational and prismatic models), and non-parametric transformations that are learned from scratch requiring minimal prior assumptions. To obtain a parameter-free description, we apply Gaussian processes (GPs) [Rasmussen and Williams, 2006] as a non-parametric regression technique to learn flexible and accurate models. To find the low-dimensional description of the moving parts, we furthermore apply a local linear embedding (LLE) [Roweis and Saul, 2000], which is a non-linear dimensionality reduction technique. As the experiments described in this paper demonstrate, our technique allows to learn accurate models for different articulated objects from real data. We regard this as an important step towards autonomous robots understanding and actively handling objects in their environment.

Throughout this paper, we consider objects that are a collection of rigid bodies denoted as "object parts" in the 3D space and that they are *articulated*, which means that the configuration of their parts can be described by a finite set of parameters. The only required input are potentially noisy observations of the poses of object parts.

2 Related Work

Learning the kinematics of robots that can actively move their own body parts has been intensively investigated in the past: Dearden and Demiris [2005] learn a Bayesian network for a 1-DOF robot. Sturm *et al.* [2008a; 2008b] proposed an approach to infer probabilistic kinematic models by learning the conditional density functions of the individual joints and by

subsequently selecting the most likely topology. Their approach requires knowledge about the actions carried out by the robot or by the observed object—information which is not available when learning the models of arbitrary, articulated objects from observations only. Similarly, Taycher *et al.* [2002] address the task of estimating the underlying topology of an observed articulated body. Their focus lies on recovering the topology of the object rather than on learning a generative model with explicit action variables. Also, compared to their work, our approach can handle higher-dimensional transformations between object parts. Kirk *et al.* [2004] extract human skeletal topologies using 3D markers from a motion capture system. However, they assume that all joints are rotational.

Yan and Pollefeys [2006] present an approach for learning the structure of an articulated object from feature trajectories under affine projections. They first segment the feature trajectories by local sampling and spectral clustering and then build the kinematic chain as a minimum spanning tree of a graph constructed from the segmented motion subspaces.

Other researchers have addressed the problem of identifying different object parts from image data. Ross *et al.* [2008] use multi-body structure from motion to extract links from an image sequence and then fit an articulated model to these links using maximum likelihood learning. There also exist approaches for identifying humans that assume a known topology of the body parts. Ramanan [2006] perform pose estimation of articulated objects from images using an iterative parsing approach. They seek to improve the feature selection to better fit the model to the image.

There exist several approaches where tracking articulated objects is the key motivation and often an a-priori model is assumed. Comport *et al.* [2004], for example, describe a framework for visual tracking of parametric non-rigid multi-body objects based on an a-priori model of the object including a general mechanical link description. Chu *et al.* [2003] present an approach for model-free and marker-less model and motion capture from visual input. Based on volume sequences obtained from image data from calibrated cameras, they derive a kinematic model and the joint angle motion of humans with tree-structured kinematics.

Similar to our approach for identifying low-dimensional articulation actions, Tsoli and Jenkins [2009] presented an Isomap-based technique that finds a low-dimensional representation of complex grasp actions. This allows human operators to easily carry out remote grasping tasks.

Katz *et al.* [2008] learn planar kinematic models for articulated objects such as 1-DOF scissors or a 3-DOF snake-like toy. They extract features from a series of camera images, that they group together to coherently moving clusters as nodes in a graph. Two nodes are connected in the graph when they are rigid. Subsequently, rotational and prismatic joints are identified by searching for rotation centers or shifting movements. In contrast to their work, we use 3D information and are not restricted to prismatic and rotation joints. We additionally can model arbitrary movements including those of garage doors which are 1-DOF actions that cannot be described by a prismatic or rotational joint. The approach of Katz *et al.* [2008] is furthermore focused on manipulation actions whereas our approach is passive and only based on observations.

3 Learning Models of Actuated Objects

In this work, we consider articulated objects consisting of n rigid object parts, which are linked mechanically as an open kinematic chain. We assume that a robot, external to the object, observes the individual parts and that it has no prior knowledge about their connectivity.

To describe the kinematics of such an articulated object, we need to reason about (i) the connections of the object parts (the topology) and (ii) the kinematic nature of the connections. Our approach seeks to find the topology and the local models that best explain the observations. We begin with a discussion of how to model the relationship of *two* object parts. The extension towards an entire graph of parts and relations is then given in Section 3.3.

3.1 Modeling the Interaction between Two Parts

The state of an object part i can be described by a vector $x_i^t \in \mathbb{R}^6$ representing the position and orientation of the part $i \in 1, \ldots, n$ at time $t = 1, \ldots, T$. We assume that only their relative transformation $\Delta_{ij} = x_i \ominus x_j$ is relevant for estimating the model, where $\oplus$ and $\ominus$ are the motion composition operator and its inverse.

If the two object parts are not rigidly connected, we assume that the articulation can be described by a latent (not observed) action variable. Examples for a latent action variable are the rotation angle of a door or the translation of a drawer. The goal is now to describe the relative transformation between the object parts using such a latent variable $a_{ij} \in \mathbb{R}^d$, where d represents the intrinsic DOF of the connection between i and j.

Since we have no prior information about the nature of the connection, we do not aim to fit a single model but instead aim to fit a set of candidate template models representing different kinds of joints. This candidate set consists of parameterized models that occur in various objects including a rotational joint ($\mathcal{M}^{\text{rotational}}$), a prismatic joint ($\mathcal{M}^{\text{prismatic}}$), and a rigid transformation ($\mathcal{M}^{\text{rigid}}$). Additionally, there may be articulations that do not correspond to these standard motions, for which we consider parameter-free models ($\mathcal{M}^{\text{LLE/GP}}$). These are computed by using a combination of the local linear embedding (LLE) dimensionality reduction technique and a Gaussian process. A more detailed description of these models is given in Section 3.4

We use a sequence of T noisy observations $z_{ij}^{1:T} = z_{ij}^1, \ldots, z_{ij}^T$ of Δ_{ij} for fitting the candidate models and for evaluating which model appears to be the best one. This is done by performing 2-fold cross-validation. In the remainder of this paper, we refer to $\mathcal{D}_{ij}$ as the training data selected from the observations, where $\mathcal{D}_{ij} \subset z_{ij}^{1:T}$, and to $\mathcal{D}_{ij}^{\text{test}}$ as the (disjoint) set of test data.

3.2 Evaluating a Model

Let $\mathcal{M}_{ij}$ be an articulation model $p(\Delta_{ij} \mid a)$ describing the connection between the part i and j and learned from the training data $\mathcal{D}_{ij}$. To actually evaluate how well an observation z_{ij} can be explained by a model, we have to determine

$p(z_{ij} \mid \mathcal{M}_{ij})$ which corresponds to

$$p(z_{ij} \mid \mathcal{M}_{ij}) = \int_a p(z_{ij} \mid a, \mathcal{M}_{ij})\, p(a \mid \mathcal{M}_{ij})\, d\,a. \quad (1)$$

The variable a is the latent action variable of the model that, for example, describes the opening angle of a door.

We assume that during the observations, there is no latent action state a that is more likely than another one, i.e., that $p(a \mid \mathcal{M}_{ij})$ is a uniform distribution. Note that this is an approximation since in our door example, one might argue that doors are more likely to be closed or completely opened compared to other states. This assumption simplifies Eq. 1 to

$$p(z_{ij} \mid \mathcal{M}_{ij}) = \int_a p(z_{ij} \mid a, \mathcal{M}_{ij})\, d\,a. \quad (2)$$

To evaluate $p(z_{ij} \mid a, \mathcal{M}_{ij})$, that is, a measure for how well model $\mathcal{M}_{ij}$ parameterized by the action variable a explains the observation z_{ij} of the part transformation Δ_{ij}, we first compute the expected transform

$$\hat{\Delta}_{ij} = \mathbb{E}_{\mathcal{M}_{ij}}[\Delta_{ij} \mid a] = f_{\mathcal{M}_{ij}}(a) \quad (3)$$

using a model-specific transformation function $f_{\mathcal{M}_{ij}}(a)$. In Section 3.4, we will specify this transformation function for all model templates. Note that we reason about the *relative* configuration between object parts here and compare the result to the observed transformation under a Gaussian error assumption with variance σ^2:

$$p(z_{ij} \mid a, \mathcal{M}_{ij}) \propto \exp\left(-||\hat{\Delta}_{ij} - z_{ij}||^2/\sigma^2\right) \quad (4)$$

To actually compute $p(z_{ij} \mid \mathcal{M}_{ij})$ using Eq. 2, we need to compute the integral over the latent action variable a. In this paper, we solve this by performing Monte-Carlo integration by sampling multiple instances of the latent variable.

Since this procedure can be rather time-consuming, we also tested an alternative strategy to approximate the integral. If we assume that $p(z_{ij} \mid a, \mathcal{M}_{ij})$ is unimodal, we can think of evaluating it only at the most likely latent action variable and approximate Eq. 2 by

$$p(z_{ij} \mid \mathcal{M}_{ij}) \quad = \quad \max_a p(z_{ij} \mid a, \mathcal{M}_{ij}). \quad (5)$$

Depending on the realization of the model $\mathcal{M}_{ij}$, we can carry out the maximization step to compute $p(z_{ij} \mid \mathcal{M}_{ij})$ efficiently.

Finally, we can compute the data likelihood for the test data set

$$p(\mathcal{D}_{ij}^{\text{test}} \mid \mathcal{M}_{ij}) = \prod_{z_{ij} \in \mathcal{D}_{ij}^{\text{test}}} p(z_{ij} \mid \mathcal{M}_{ij}). \quad (6)$$

3.3 Finding the Connectivity

So far, we ignored the question of connectivity and described how to evaluate a model $\mathcal{M}_{ij}$ representing a connection between the parts i and j. If we consider the individual object parts as nodes in a graph and the connections as edges between nodes, then the set of possible acyclic object structures that connect all parts is given by all spanning trees of this graph. The endeavor of explicitly computing, evaluating, and reasoning with all possible topologies, however, results in an intractable complexity. We therefore seek to find the *spanning tree* $\mathbb{M}$ that results in a combined model for all object parts that both maximizes the expected data likelihood of a new observation, i.e.,

$$p(\mathcal{D}^{\text{test}} \mid \mathbb{M}) = \prod_{\mathcal{M}_{ij} \in \mathbb{M}} p(\mathcal{D}_{ij}^{\text{test}} \mid \mathcal{M}_{ij}), \quad (7)$$

while at the same time minimizing the overall complexity of the combined model. The latter is calculated in a fashion similar as with the Bayesian information criterion. In our case, we measure the model complexity by the dimensionality of the latent action space.

To find this topology (that is, the spanning tree of the local models), we fit for all tuples of rigid parts all models from the candidate template model set and add for each model a link to the graph. We then assign to each edge in the graph the cost of model $\mathcal{M}_{ij}^{\text{type}}$ that is equal to the negative expected data log-likelihood plus a complexity penalty of the model:

$$\text{cost}_{\mathcal{M}_{ij}^{\text{type}}} = -\frac{1}{\|\mathcal{D}^{\text{test}}\|} \log p(\mathcal{D}^{\text{test}} \mid \mathcal{M}_{ij}^{\text{type}}) + C(\mathcal{M}_{ij}^{\text{type}}) \quad (8)$$

Then, the task of finding the topology of local models which minimize this cost function is equivalent to finding the minimal spanning tree in this graph which can be done rather efficiently.

Please note that the resulting kinematic tree can be transformed into a Bayes net (BN) by replacing the edges by connected nodes representing local models $\mathcal{M}$ and latent action variables a and by adding nodes for (absolute) object part observations and relative observations z. The resulting BN naturally encodes all independence assumptions made in our work. Such a BN, however, is complex and hard to visualize. We therefore stick at this point to a graph-like visualization as shown in the left image of Fig. 2. Bold arrows indicate the selected models form the spanning tree structure. The plot in the middle illustrates the prediction error of all considered models during learning. The right image depicts the probability density function of the model $\mathcal{M}^{\text{LLE/GP}}$.

3.4 Model Templates

This section explains the instances of the set of candidate model templates.

Rigid Transformation Model

The simplest connection between two parts is a rigid transformation without any latent action variable. The model-specific transformation function of Eq. 3 for the rigid transform model $\mathcal{M}^{\text{rigid}}$ from training data $\mathcal{D}$ then reduces to the estimating the mean, i.e.,

$$f_{\mathcal{M}_{ij}^{\text{rigid}}} = \frac{1}{\|\mathcal{D}_{ij}\|} \sum_{z_{ij} \in \mathcal{D}_{ij}} z_{ij}. \quad (9)$$

Prismatic Joint Model

For modeling prismatic joints that can be, for example, found in a drawer, we assume a 1-DOF latent action variable that describes the motion between the object parts. Prismatic joints

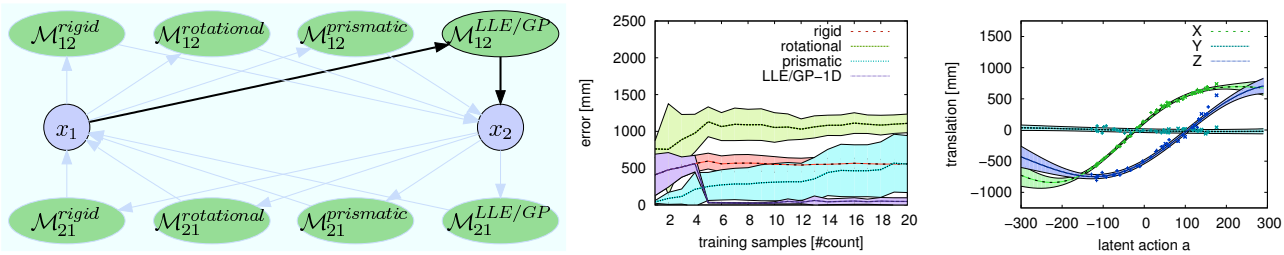

Figure 2: Learning the kinematic model for a garage door. Left: The fully connected graph contains instantiations of all possible template models and the selected models are indicated by bold arrows. Middle: evolution of the data likelihood of different models. Right: transformation function learned by the LLE/GP model.

move along a single axis, that can for example be found using principle component analysis. Internally, we model the action a_{ij}^t as the relative movement with respect to the first observation z^1 in $\mathcal{D}$ (therefore $a_{ij}^1 = 0$) along its principal axis e of unit length. Let $trans$ be the function that removes all rotational components, we obtain:

$$\hat{a}_{ij}^t = e \cdot trans(\Delta_{ij}^t - \Delta_{ij}^1) \tag{10}$$

The model-specific transformation function for the prismatic model $\mathcal{M}^{\text{prismatic}}$ then becomes

$$f_{\mathcal{M}_{ij}^{\text{prismatic}}}(a) = ae + \Delta^1. \tag{11}$$

Rotational Joint Model

In the case of a rotational joint, we compute the latent 1-DOF action variable from Eq. 5 by taking the first observation as a reference (similar as in the prismatic joint model). The rotational components describe a line, whose direction e can be found by principle component analysis. We computing the angular difference of all observations relative to the first one

$$\hat{a}_{ij}^t = e \cdot angle(\Delta_{ij}^t - \Delta_{ij}^1). \tag{12}$$

Here, $angle$ is a function that removes all non-rotational components.

Since our model assumes a 1-DOF latent action variable, the positions of the observed parts describe a circular arc or a single point in case the observed object part lies on the axis of rotation. By standard geometric operations, we estimate the axis of rotation $n \in \mathbb{R}^3$, the rotational center $c \in \mathbb{R}^3$, and the rigid transform $r \in \mathbb{R}^6$ carried out after the rotation. Then, the model-specific transformation function for the rotational model $\mathcal{M}^{\text{rotational}}$ becomes

$$f_{\mathcal{M}_{ij}^{\text{rotational}}}(a) = [c; n]^T \oplus rot_Z(a) \oplus r, \tag{13}$$

where $rot_Z(a)$ describes a rotation about the Z axis by a and $\oplus$ is the motion composition operator.

LLE/GP Joint Model

Although rigid transformations in combination with rotational and prismatic joints might seem at the first glance to be sufficient for a huge class of kinematic objects, it turns out that many real-world objects lack a clear shifting or rotation axis. One example for such objects is a garage door. Therefore, our candidate model template set contains one non-parametric model that is able to describe general transformations. This model is based on non-linear dimensionality reduction via local linear embedding for discovering the latent action manifold and a Gaussian process regression to learn a generative model.

Consider the manifold that is described by the observations of object poses in $\mathcal{D}_{ij} = \Delta_{ij}^1, \ldots, \Delta_{ij}^T$ for the link between rigid part i and j. Depending on the DOF d of this particular link, all data samples will lie on or close to a d-dimensional manifold with $1 \leq d \leq 6$ being non-linearly embedded in $\mathbb{R}^6$. There are many dimensionality reduction techniques such as PCA for linear manifolds or Isomap [Tenenbaum *et al.*, 2000] and LLE [Roweis and Saul, 2000] for non-linear manifolds. Our current implementation applies LLE but is not restricted to this method. LLE first expresses each data point as a linear combination of its neighbors, here in $\mathbb{R}^6$, and then computes a low-dimensional representation in $\mathbb{R}^d$ satisfying the identical linear relationships.

In more detail, LLE first finds the k-nearest neighbors of each data sample Δ^t in $\mathcal{D}$ (we neglect the indices i and j for a better readability here). For each data sample, LLE then computes a vector of weights that best reconstructs the data sample Δ^t from its neighbors. Let W be the weight matrix for all samples. LLE seeks for the weight matrix that minimizes the reconstruction error ε given by

$$\varepsilon(W) = \sum_t \|\Delta^t - \sum_{t'} W_{tt'} \Delta^{t'}\|^2. \tag{14}$$

By normalization, we require that the reconstruction weights for each data sample t to sum to one over its neighbors, i.e., $\sum_{t'} W_{tt'} = 1$. Minimizing Eq. 14 can be achieved via Lagrange minimization in closed form.

After determining the reconstruction weight matrix, LLE seeks for a point-wise mapping of each data sample Δ^t to a local coordinate a^t on the d-dimensional manifold. This mapping has to ensure that the weight matrix W reconstructs also the local coordinates of the data samples on the manifold. This is done by searching for the local coordinates $a^1, \ldots, a^T$ for $\Delta^1, \ldots, \Delta^T$ so that the reconstruction error Ψ

$$\Psi(a^1, \ldots, a^T) = \sum_t \|a^t - \sum_{t'} W_{tt'} a^{t'}\|^2, \tag{15}$$

on the manifold is minimized.

With a few additional constraints, the minimization of Eq. 15 can be solved as a sparse $T \times T$ eigenvector problem.

The local coordinates are then computed based on the eigenvectors. For further detail, we refer the reader to Roweis and Saul [2000].

The reconstructed latent action values can now be used for learning $p(z \mid a, \mathcal{M})$ from the training data $\mathcal{D}$. In our work, we employ Gaussian process regression, which is a powerful and flexible framework for non-parametric regression. For the sake of brevity, we refer the interested reader to Rasmussen and Williams [2006] for details about GP regression.

4 Experiments

To evaluate our approach, we recorded observations from two typical household objects, a microwave door and a cabinet with two drawers. To track the poses and orientations of the parts, we placed the objects in a PhaseSpace motion capture studio. For each object, we recorded 200 data samples while manually articulating the object. Additionally, we simulated a garage door as a typical object that cannot be described using a prismatic or rotational joint. We also estimated the model of a table moved on the ground plane to give an example of latent action variables with more than one dimension.

Our experiments are designed so that we can recover accurate transformation models for each link between parts along with the kinematic structure. In addition, we show that the range of the latent action space can be estimated and configurations of this range can be generated for visual inspection.

Model Selection

We evaluated the prediction accuracy and the expected data likelihood for each of the microwave, the drawer, and the garage door dataset for all models of out candidate set. For the evaluation, we carried out 10 runs and in each run, 40 observations were drawn independently and randomly from the data set, 20 of them were used for learning and 20 for testing. The quantitative results showing the prediction error of the models are depicted in Tab. 1. As can be seen, the flexible LLE/GP model can fit all objects well.

As can be seen from the table, the rotational model predicts best the opening movement of the microwave door while the prismatic model predicts best the motion of the drawer which is the expected result. It should be noted that the LLE/GP model is only slightly worse than the parametric models and is able to robustly predict the poses of the door and the drawer (1.1mm vs. 1.5mm for the microwave, and 0.7mm vs. 3.6mm for the drawer).

In the case of the garage door, however, all parametric models fail whereas the LLE/GP model, designed to describe general transformations, provides accurate estimates. Here we evaluated different levels of noise, and found that the LLE/GP model to be quite robust. Fig. 3 illustrates the motion of the garage door estimated by the non-parametric model. Note that our models also encode the range of the latent action variable a learned from observations.

This experiment shows that our system takes advantage of the expert-designed parametric models when appropriate while keeping the flexibility to also learn accurate models for unforeseen mechanical constructions.

dataset	error of $\mathcal{M}^{\text{rotational}}$		error of $\mathcal{M}^{\text{prismatic}}$		error of $\mathcal{M}^{\text{LLE/GP}}$	
microwave	**1.1mm** ±0.2mm	**0.1°** ±0.1°	65.9mm ±13.7mm	23.1° ±2.2°	**1.5mm** ±1.7mm	**0.2°** ±0.2°
drawer	67.2mm ±24.4mm	1.6° ±0.4°	**0.7mm** ±0.1mm	**0.9°** ±0.1°	**3.6mm** ±6.2mm	**0.6°** ±0.1°
garage door (no noise)	1059.4mm ±147.4mm	0.0° ±0.0°	382.3mm ±265.0mm	25.1° ±3.9°	**8.5mm** ±9.2mm	**0.4°** ±0.4°
(noise $.1\sigma$)	1052.6mm ±146.1mm	0.2° ±0.0°	507.7mm ±353.1mm	25.0° ±3.7°	**18.2mm** ±27.1mm	**0.9°** ±1.3°
(noise 1σ)	1108.3mm ±126.6mm	2.6° ±1.0°	555.9mm ±387.4mm	26.5° ±3.4°	**47.9mm** ±49.2mm	**2.8°** ±2.2°
(noise 10σ)	934.4mm ±289.4mm	27.4° ±11.8°	510.5mm ±239.2mm	28.9° ±1.8°	**248.3mm** ±24.1mm	**16.5°** ±1.8°

Table 1: Average prediction error and standard deviation of local models on test data over all runs. Gaussian noise with $\sigma = (10\text{mm}, 1°)$ was added to the garage door data.

Structure Discovery

A typical articulated object consisting of multiple parts is a cabinet with drawers as illustrated in the left image of Fig. 4. In the experiment, we obtain pose observations of three rigid parts x_1, x_2, and x_3. First, we opened and closed only the lower drawer. Accordingly, a prismatic joint model is learned for link Δ_{13} (see top left image of Fig. 4). When also the upper drawer gets opened and closed, the rigid transform at Δ_{12} is replaced by a second prismatic joint model $\mathcal{M}^{\text{prismatic}}$, resulting in a kinematic tree. As a second multi-part object we present a yard stick, consisting of four consecutive elements with three rotational links, as depicted in Fig. 5. These experiments demonstrate that by using the data likelihood for selecting the minimum spanning tree we are able to infer the correct kinematic structure.

Multi-dimensional Latent Action Spaces

To illustrate that our approach is also able to find the models with a higher-dimensional latent action variable, we let the robot monitor a table that was moved on the ground plane. The robot is equipped with a monocular camera tracking a marker attached to the table. In this experiment, the table was only moved and was never turned, lifted, or tilted and therefore the action variable will have 2-DOF. Fig. 6 shows four snapshots during learning. Initially, the table is perfectly explained as a rigid part of the room (top left). Then, a prismatic joint model best explains the data since the table was moved in one direction only (top right). After moving sideways, the best model is a 1-DOF LLE/GP that follows a simple curved trajectory (bottom left). Finally full planar movement is explained by a 2-DOF LLE/GP model (bottom right).

Simplified Likelihood Computation

To evaluate the likelihood of a model one has to integrate over the latent variable a (see Eq. 2) which is done via Monte-Carlo integration. If we instead use the approximation shown in Eq. 5, we only need to evaluate one single action variable. In our current implementation, this speeds up the required computation time by a factor of 100 while both approaches select the same model. Even though the actual values for the likelihood differ slightly, we were unable to produce a dataset in which both strategies select different models.

5 Conclusions

In this paper, we presented a novel approach for learning kinematic models of articulated objects. Our approach infers the connectivity of rigid parts that constitute the object

including the articulation models of the individual links. To model the links, our approach considers both, parameterized as well as parameter-free representations. It combines non-linear dimensionality reduction and Gaussian process regression to find low-dimensional manifolds that best explain the observations. Our approach has been implemented and tested using real data. In practical experiments, we demonstrated that our approach enables a robot to infer accurate articulation models for different everyday objects.

References

[Chu *et al.*, 2003] C.-W. Chu, O.C. Jenkins, and M.J. Matarić. Markerless kinematic model and motion capture from volume sequences. In *CVPR*, 2003.

[Comport *et al.*, 2004] A.I. Comport, E. Marchand, and F. Chaumette. Object-based visual 3d tracking of articulated objects via kinematic sets. In *Workshop on Articulated and Non-Rigid Motion*, 2004.

[Dearden and Demiris, 2005] A. Dearden and Y. Demiris. Learning forward models for robots. In *IJCAI*, 2005.

[Katz *et al.*, 2008] D. Katz, Y. Pyuro, and O. Brock. Learning to manipulate articulated objects in unstructured environments using a grounded relational representation. In *Robotics: Science and Systems*, 2008.

[Kirk *et al.*, 2004] Adam Kirk, James F. O'Brien, and David A. Forsyth. Skeletal parameter estimation from optical motion capture data. In *SIGGRAPH*, 2004.

[Ramanan, 2006] D. Ramanan. Learning to parse images of articulated bodies. In *NIPS*, 2006.

[Rasmussen and Williams, 2006] C.E. Rasmussen and C.K.I. Williams. *Gaussian Processes for Machine Learning*. The MIT Press, Cambridge, MA, 2006.

[Ross *et al.*, 2008] David A. Ross, Daniel Tarlow, and Richard S. Zemel. Unsupervised learning of skeletons from motion. In *ECCV '08*, 2008.

[Roweis and Saul, 2000] S.T. Roweis and L.K. Saul. Nonlinear dimensionality reduction by locally linear embedding. *Science*, 290(5500):2323–2326, 2000.

[Sturm *et al.*, 2008a] J. Sturm, C. Plagemann, and W. Burgard. Adaptive body scheme models for robust robotic manipulation. In *Robotics: Science and Systems*, 2008.

[Sturm *et al.*, 2008b] J. Sturm, C. Plagemann, and W. Burgard. Unsupervised body scheme learning through self-perception. In *ICRA*, 2008.

[Taycher *et al.*, 2002] L. Taycher, J.W. Fisher III, and T. Darrell. Recovering articulated model topology from observed rigid motion. In *NIPS*, 2002.

[Tenenbaum *et al.*, 2000] J.B. Tenenbaum, V. de Silva, and J.C. Langford. A global geometric framework for nonlinear dimensionality reduction. *Science*, 290(5500):2319–2323, 2000.

[Tsoli and Jenkins, 2009] A. Tsoli and O.C. Jenkins. Neighborhood denoising for learning high-dimensional grasping manifolds. In *IROS*, 2009.

[Yan and Pollefeys, 2006] J. Yan and M. Pollefeys. Automatic kinematic chain building from feature trajectories of articulated objects. In *CVPR*, 2006.

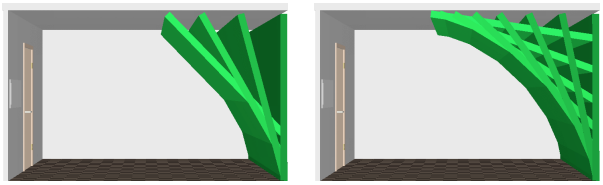

Figure 3: Motion of a garage door predicted by our non-parametric model. Left: Model after the first few observations. Right: after processing all observations.

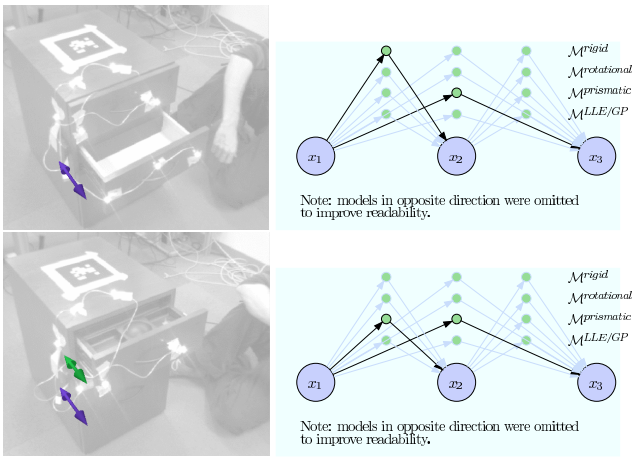

Figure 4: Estimating a model of two drawers of a cabinet. Top: initially, only the lower drawer is opened and closed and the corresponding kinematic structure is inferred. Bottom: both drawers are opened and closed independently.

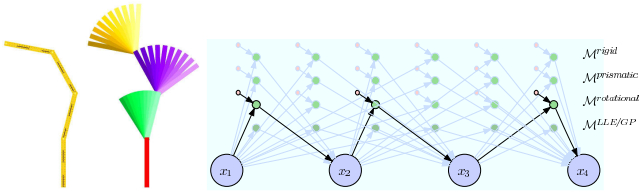

Figure 5: simulated yard stick consisting of 4 consecutive elements. Model selection correctly reveals the sequential chain.

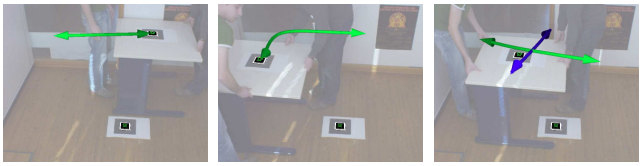

Figure 6: Learning a model for a table moving on the ground plane. Arrows indicate the dimensions of the latent action.